Combined local anodization of titanium and scanning photoelectrochemical mapping of TiO2 spot arrays

Vasilica Badets, Gabriel Loget, P. Garrigue, N. Sojic, D. Zigah

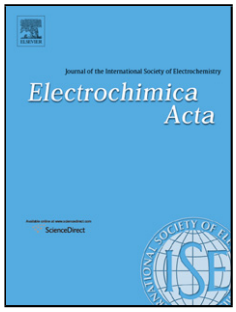

Title: Combined local anodization of titanium and scanning photoelectrochemical mapping of TiO_2 spot arrays

Author: V. Badets G. Loget P. Garrigue N. Sojic D. Zigah

PII: S0013-4686(16)32254-X
DOI: http://dx.doi.org/doi:10.1016/j.electacta.2016.10.151
Reference: EA 28239

To appear in: *Electrochimica Acta*

Received date: 16-5-2016
Revised date: 20-10-2016
Accepted date: 22-10-2016

Please cite this article as: V.Badets, G.Loget, P.Garrigue, N.Sojic, D.Zigah, Combined local anodization of titanium and scanning photoelectrochemical mapping of TiO2 spot arrays, Electrochimica Acta http://dx.doi.org/10.1016/j.electacta.2016.10.151

Combined local anodization of titanium and scanning photoelectrochemical mapping of TiO_2 spot arrays

V. Badets,[a,c] G. Loget,[b] P. Garrigue,[a] N. Sojic,[a] D. Zigah[*a]

[a] *Univ. Bordeaux, ISM, CNRS UMR 5255, F-33400 Talence, France*

[b] *Univ. Rennes 1, ISCR, CNRS UMR 6226, 35042 Rennes, France*

[c] *Université de Strasbourg, CNRS, CHIMIE UMR 7177, F-67000 Strasbourg, France*

Graphical abstract

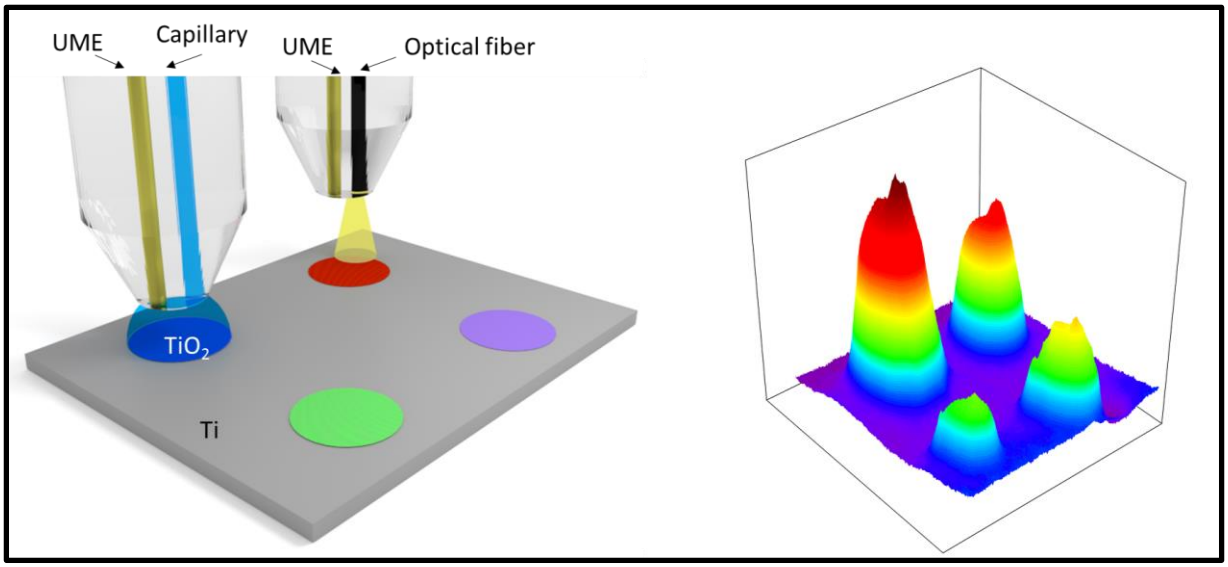

Abstract

Localized growth of TiO_2 and rapid screening of TiO_2 photoelectrochemical properties by scanning electrochemical microscopy (SECM) are described. We report the fabrication and operation of an electrochemical tool comprising a microcapillary and an ultramicroelectrode (Cap-UME) that is used for the local formation of TiO_2 microspots. This tip allows the generation of arrays of TiO_2 of different physicochemical and catalytic characteristics. Moreover, these results prove that local anodization is an efficient method to obtain TiO_2 films with micrometre resolution. The use of a combined optical fibre-ultramicroelectrode (OF-UME) in a SECM configuration may operate in two different detection modes. In the first mode, the array is biased and the OF-UME is used as a scanning light source allowing a photocurrent

mapping of the surface. In the second mode, the dual OF-UME system serves simultaneously as a light source and an O_2 electrochemical sensor which resolved spatially the photoelectrochemically generated O_2 species. A direct correlation between the potentials used to produce TiO_2, the photocatalytic properties of the TiO_2 spots and the amount of oxygen produced was found, demonstrating the strong potential of these tools for the rapid and convenient mapping of TiO_2 array properties on a single surface.

Keywords: local anodization, scanning electrochemical microscopy, photoelectrochemistry, microcapillary, ultramicroelectrode, optical fibre, titanium dioxide

1. Introduction

Because of its chemical stability, electronic properties and biochemical compatibility, titanium dioxide is one of the most important semiconductor for a wide variety of applications, such as dye-sensitized solar cells, photocatalysis and medical implants [1, 2]. It is well-known that the properties of TiO_2 surfaces strongly depend on their structures and consequent efforts were focused on the optimization of TiO_2 layers in order to achieve the optimal performances for a given application [3, 4]. In many of these applications, a high specific surface area is required for achieving a high overall efficiency and therefore, TiO_2 nanoparticles are widely synthesized. Among various existing synthesis methods, such as template-assisted methods, sol–gel methods, or hydro/solvothermal approaches, electrochemical means and especially electrochemical anodization of a metallic titanium surface is a low-cost one-step method that yields a easy to handle TiO_2 layer, already electrically connected to the surface. Under right experimental conditions, the most spectacular shape among the 1D structures of TiO_2, namely self- organised nanotubes, can be obtained. Anodization is currently performed on large Ti substrates, having an area in a cm^2 range, but little attention was given to micro [5] or nano-electrochemical oxidation of Ti plates. In the work of Vullers *et al* [6] and Ozcan *et al* [7] a AFM tip was used for the local generation of nanometric TiO_2 lines on a Ti plate for the development of single electron transistor, but no further morphological characterisation of the oxide was given. TiO_2 spots in a micrometer and millimeter range were produced by scanning droplet technique, but using only buffered aqueous electrolyte [8, 9]. The anodization was performed in a rather low potential range (4 to 18 V) and no characterisation of the photochemical properties of the TiO_2 spots was given. Apart the electrochemical anodization, micropatterning a substrate with TiO_2 was recently proposed using hydrothermal synthesis [10,

11]. The procedure consists of preparing the pattern by combining self-assembled monolayer and UV lithography or stamping [12]. The Ti^{4+} salt is hydrolysed in acidic conditions and TiO_2 is deposited as anatase form on the entire surface. Lift-off is the final step required to achieve a micropattern containing only TiO_2 with a specific morphology.

In this view, this work presents the local electrochemical anodization of Ti in an organic electrolyte, as an alternative one-step process to obtain micropatterns of TiO_2. The formation of TiO_2 oxide layer results of the oxidation of Ti to Ti^{4+} (equation 1) and its reaction with water (equation 2). Fluoride ions are used to form a soluble hexafluorotitanium complex $[TiF_6]^{2-}$ that leads to a porous structure with enhanced photocatalytic activity (equation 3) [13].

$$Ti \rightarrow Ti^{4+} + 4e^- \quad (1)$$

$$Ti^{4+} + H_2O \rightarrow TiO_2 + 4H^+ \quad (2)$$

$$TiO_2 + 6F^- + 4H^+ \rightarrow [TiF_6]^{2-} + 2H_2O \quad (3)$$

Our aim is first to show that the local anodization of Ti in an organic electrolyte is able to yield sub-millimetre and micrometre diameter TiO_2 spots having different photocatalytic properties; and then, to demonstrate the utility of these arrays for screening the catalytic properties of TiO_2 layers with different morphologies. To achieve these goals, an anodization tool was developed, the Cap-UME (Figure 1) that is composed of a microcapillary part combined to a gold ultramicroelectrode (UME). The micrometre size of the writing tip of the Cap-UME scales down the classical anodization cell to a droplet-sized cell where the gold UME serves as a cathode and the electrolyte is dispensed through the microcapillary. In these conditions, the anodization is performed only in the sub-microliter droplet and the surface of the generated TiO_2 layer is in the micrometre range (Figure 1). The presented system benefits of all the advantages of the classical anodization such as its low cost and easy implementation. The advantage of the local anodization over the classic anodization is the possibility to obtain on the same Ti substrate TiO_2 films with different photocatalytic properties by controlling the anodization potential and time. Scanning electrochemical microscopy (SECM) is a scanning probe microscopy technique that enables local electrochemical measurement on a micrometer scale. In SECM configuration the movement of an UME along the three-axis (x, y, z) is possible using stepper motors controller. The probe can scan a substrate immersed in an electrolyte solution. SECM is used for several years to locally investigate photoelectrochemical reaction [14-17]. For the screening of the modified surfaces, a new original tool composed of an optical

fibre and a gold UME (OF-UME) is described and operated. This movable tip scans the entire Ti surface and gives simultaneous information about the produced photocurrent for water oxidation and about the oxygen produced during this reaction.

2. Experimental

2.1. Fabrication of microcapillary-ultramicroelectrode tool

A borosilicate theta-capillary (TST150-6, World Precision Instruments) was used for the fabrication of the microcapillary-ultramicroelectrode tool. A nickel and a gold wire (from Goodfellow), both with a diameter of 50 µm and a length of 3 cm, were inserted in a 15 cm long theta capillary. The final gold electrode, with a diameter of 50 µm, can be classified as UME [18]. The assembly containing the theta capillary and the two wires was placed in the chamber of a laser based micropipette puller (Sutter instruments P2000) and thinned using a single line programme (Heat 600, Filament 5, Velocity 40, Delay 120, Pull 5, and Time 15 seconds). Sealing of the wires is performed using a single line programme (Heat 600, Filament 5, Velocity 40, Delay 120, Pull 0, and Time 50 seconds) while two stoppers are placed on the pullers bars to avoid the weak pulling forces that could further thin and break the capillary. Finally, after removing the stoppers, a pulling program (Heat 900, Filament 1, Velocity 40, Delay 120, Pull 25) separates the two sides of the capillary. The extremity of the obtained devices was polished with sand paper and alumina suspension (0.3 and 0.05 µm). At this stage, the obtained tool is similar to double UME composed of a Ni and Au microelectrodes. For removing the Ni wire, the tool was placed in a concentrated solution of HNO_3 for 3 days. After the total dissolution of Ni wire and final rinsing with Milli-Q water, an empty microcapillary with a diameter of 50 µm is obtained. The new tool is measuring 300 µm in diameter and it is composed of capillary and Au ultramicroelectrode (subsequently named Cap-UME, Figure 1a and b). For the electrical contact, carbon powder and a copper wire are inserted in the compartment of the Au UME.

2.2. Localized anodization of Ti substrate using the microcapillary-ultramicroelectrode tool

The microcapillary part of the new tool (Cap-UME) was filled with the electrolyte solution required for the anodization. This solution was composed of ethylene glycol containing 1.5 M lactic acid, 0.1 M ammonium fluoride and 5% water [19]. All the chemicals were purchased from Sigma-Aldrich. The Cap-UME was placed in the holder of the scanning electrochemical microscopy SECM setup (CH Instruments, Texas Model 920C) [20]. The SECM cell contains

a Ti plate (Alfa Aesar, size 1 cm x 1 cm, thickness 250 µm). In a two-electrode configuration, where the Au UME is the cathode and the Ti plate is the anode, a potential of 0.5 V was applied while the Cap-UME was approached to the surface with a speed of 1 µm s^{-1}. When the tool is close to the surface, the hanging meniscus of the Cap part touches the surface and closes the circuit between the anode and the cathode. A current jump is therefore recorded and used to automatically stop the movement of the Cap-UME tip (figure S1). After positioning the tip, the local anodization of the Ti plate was performed in a two-electrode configuration. An external power sources (Heinzinger PNC 600-1000 pos) was used for the polarisation of the Ti plate within the range of 50 to 125 V. After a first local anodization at 50 V, the Cap-UME tip was lifted up and repositioned in a different location for a new anodization. Anodization time of one hour was used in all the experiments if not mentioned otherwise. The approach sequence is repeated and a new anodization is performed using the desired potential (75, 100, 125 V). Local spots of TiO_2 are hence obtained (figure 1c). After dipping the Ti/TiO_2 plate in ethanol overnight to remove the fluorides, annealing was performed in air at 400°C for 1 hour, with a ramp of 30°C min^{-1}. This procedure assures the conversion of TiO_2 to an anatase phase, required for an optimal photoelectrochemical activity [21-23].

2.3. Fabrication of optical fibre-ultramicroelectrode tool

An optical fibre (diameter 50 µm, cladding 120 µm, length 2 m, Thorlabs, FG050UGA, Multimode Fiber, 0.22 NA) and a gold wire (diameter 25 µm, length 3 cm) were placed in a borosilicate capillary. The assembly was placed in the chamber of a laser based micropipette puller. The same procedures of thinning, sealing, pulling, polishing and electrical contacting were employed as described previously for the Cap-UME tool. Finally, the tip (diameter 500 µm, figure 2a) composed of an optical fibre touching an Au ultramicroelectrode (subsequently named OF-UME) was obtained and further used for measuring the photoelectrochemical activity of the TiO_2 spots. On figure S2a and S2b the optical fiber it is respectively without and with illumination, the yellow disc is the gold ultramicroelectrode.

2.4. SECM simultaneous screening using the optical fibre-ultramicroelectrode tool

The OF-UME tool was employed in a three-electrode configuration, where the Au UME was the working electrode (WE1), an Ag/AgCl, NaCl 3 M was the reference electrode and a Pt wire was the counter electrode. A SECM-bipotentiostat served to apply a potential E_{sub} = 0.5 V to the Ti plate that acted as a second working electrode (WE2) [24]. The electrolyte was 1 M NaOH. The optical fibre was coupled to a mercury-xenon lamp (LC8 from Hamamatsu), the illumination power on the Ti/TiO_2 substrate was about 100 mW cm^{-2} and the size of the light

spot on the surface is estimated to be 4.6 x 10^{-3} mm^2 (calculation detail in SI). The OF-UME tool was moved along xy axes at a scan rate of 400 µm s^{-1} while the UV source was turned on, illuminating locally the Ti plate. The current of the Ti plate was recorded continuously; however the photoelectrochemical oxidation of water was monitored only above a TiO_2 spot. In this manner, a 2D image of Ti plate containing the TiO_2 spots was obtained. On these images, the normalized current was represented, it is the substrate current divided by the current recorded above the Ti. In parallel, the current of the Au UME was recorded. Preliminary experiments performed of a macroscopic TiO_2, allowed us to determine the tip potential for O_2 reduction which occurs at E_{UME} = -0.4 V vs Ag/AgCl. Therefore, this potential was imposed for O_2 detection during the scanning experiments. When the biased OF-UME was above a TiO_2 spot, the current recorded at the UME corresponds to the reduction of O_2 produced during the oxidation of H_2O at the TiO_2 spot. Hence, the OF-UME allows the simultaneous measurements of the photoelectrochemical activity on the Ti plate and of the oxygen reduction on the Au UME (figure 2b).

3. Results and discussion

3.1. Fabrication and Characterization of Cap-UME and OF-UME

A Cap-UME consists of a microcapillary and an ultramicroelectrode built in the same theta capillary (figure 1a). When the microcapillary was filled with solution, a liquid meniscus covered also the Au UME allowing the formation of a small electrochemical droplet cell when the drop touched the surface of Ti plate (figure S1).

Similar approaches have been developed in the literature. For instance, a combined capillary-carbon nanoelectrode was recently developed by Takahaski *et al.* [25-28] and used as combined SECM with scanning ion conductance microscopy (SICM). Although the nano-features of this electrode could present an interest for obtaining sub-micrometer TiO_2 spots, the risk of carbon incorporation in the TiO_2 film could lead to a change in the film composition and morphology [29]. For this reason, gold electrode was chosen for the construction of our system.

In an attempt to reduce the size of the TiO_2 spots, a classical capillary was thinned down to a diameter of 20 µm. A gold wire and the electrolyte were inserted in upper part of the capillary [28]. The setup was approached to the Ti plate using the procedure described in figure S1. Although the anodization was possible, this tool was fragile and broke easily. As a consequence, the electrolyte leaked and final size of the spot was high and not reproducible. For these reasons,

the Cap-UME was fabricated as a robust tool with a diameter of 300 µm, allowing a good reproducibility of the spot size.

The OF-UME is an optical fiber sealed with a gold wire in the same capillary (figure 2). On the SEM image of the OF-UME, the shinning disc is the gold UME and in the vicinity is located the optical fiber (figure 2a). On the optical image of the OF-UME (figure S2a,b) it was possible to observe the optical fiber when the light is turned off and on. A typical characterisation of the Au UME was performed beforehand by recording a cyclic voltammogram in an electrolytic solution containing ferrocenedimethanol. The classic sigmoidal shape of an UME at low scan rates was obtained with a plateau current very similar to the theoretical one corresponding to a microelectrode of a diameter of 25µm (figure S3) and no influence of the UV light irradiated from the fibre could be observed. This confirms that the fabrication process of the OF-UME tool is suitable for obtaining high-quality UME with an intact disk shape and that the UME operates without interferences of UV light. The principle of combining UME with an optical fiber has been around for several years. Bard *et al.* [30] used an optical fiber coated with gold and encased in an outer electrophoretic insulating sheath to obtain a ring electrode. The fabrication method was tedious and involved several steps such as (1) heating and pulling of the optical fibers, (2) metal coating, (3) electrical insulation, and (4) exposure of the electrode at the end of the tip. Smyrl *et al.* [31] used another system where they coated an optical fiber with gold. The disadvantage of this method resides in the difficulty of obtaining a gold layer thin enough to transmit UV light but thick enough to be stable during all the SECM experiment. Even if the concept of optical-microelectrode is described in the literature, the construction of the OF-UME presented in this work is much simpler and more straightforward.

3.2. TiO_2 spots produced via the local anodization of Ti

The Cap-UME was used for the local growth of four different TiO_2 spots on the same surface at different anodization potentials. Figure S4a shows an optical image of the TiO_2 spots obtained on the Ti plate. Each spot displays a distinct colour due to a different thickness of the TiO_2 layer [32, 33] .Because of the small diameter of the spots, it was not possible to obtain a cross section of the TiO_2 that allows estimating the thickness. Ellipsometry is another technique that could give information about the thickness of TiO_2 layers, but since the Ti substrate was not polished prior the anodization, accurate measurement could not be achieved. Moreover, due to the different morphologies and porosity of each TiO_2 spots, a lot of inaccurate assumptions

in the creation of the model required for ellipsometry measurements would have led to hazardous values of the thickness. However, since it is well known that the thickness of TiO_2 increases with the applied potential, the obtained colours (yellow, violet-blue, pale aqua and pale purple) correspond to films thicknesses varying from 30 to 100 nm [33]. The sizes of the spots increased from 450 µm to 750 µm with the higher values of the anodization potential. The increase of the anodization potential induces an increase in the anodization current (Figure S5). As the electrolyte solution is located in the microcapillary whereas the cathode (gold UME) is adjacent to the microcapillary, an increase in the anodization current induces a stronger electromigration that expands the volume of the droplet and thus, the spot size is correlated with the anodization potential. Moreover, as mentioned elsewhere, surface tension increases also with the anodization potential, leading to an increase on the spots size [34]. On each individual spot, the existence of a central region with a different colour than the rest of the spot can be observed, suggesting a radial thickness gradient. These results are explained by the fact that the strongest electric field intensity is located below the UME [35]. These observations are confirmed by the low magnification SEM images in Figure S4b. The size of each central region (pictured in white colour) is 70, 80, 100 and 180 µm according to increasing anodization potential of 50, 75, 100 and 125 V, respectively. The images reveal also the existence of a middle region (light grey) and an external region (dark grey) corresponding to a TiO_2 layer with a thickness decreasing from the centre to the outer part of the spot. Even if such conditions were initially expected to yield TiO_2 nanotubes [19], the formation of a porous structure can be explained by local change of pH under the UME. Indeed, the reduction of water at the UME leads to a local pH increase that can drastically disturb the formation of nanotubes [36].

The morphological characterisation of the TiO_2 spots was followed by the measurement of the photoelectrochemical activity. This was achieved using the OF-UME system (see the experimental part for the fabrication procedures). Figure 3 shows the photoelectrochemical activity of the four TiO_2 spots. It can be observed that the photocatalytic current increases with the anodization potential. This is explained by a larger amount of holes generated on TiO_2 due to the increase of the surface area when the thickness increases. Such a correlation applies because of the high porosity of the film. Also, for each individual spot, a gradient from its centre to its external part identified in the SEM images is well revealed also by the photocurrent that decreases from the centre to the exterior of the spot. Therefore, the variation of the catalytic current within a single spot is correlated with the assumed radial variation of the thickness of TiO_2 from the centre to the exterior of the spot.

High magnification SEM images were recorded in the centre of each spots, corresponding to the highest catalytic activity. Figure 4 shows an amorphous structure for the spot at 50 V, a structure containing an early phase of TiO_2 nanotubes growth for the spot at 75 V and a nanoporous structure with pore size around 30 nm for the spots at 100 V and 125 V. The structures in the centre of the spot and the surroundings (Figure S6) are different. However, the photocatalytic current remains almost constant. Therefore, the photocatalytic activity likely depends on the assumed thickness of the TiO_2 layer which increases with the anodization potential and does not depend on the morphology of the layer.

The effect of extended anodization time (4 hours) on the morphology and photocatalytic current is shown in Figure 5. The spot obtained at 50 V is composed of low ordered nanotubes of TiO_2 and the spot at 75 V consists of a nanoporous structure. While the photocurrent did not significantly changed with the increase in the anodization time, these results show that the size of the TiO_2 spots considerably increased with the time, leading to spots with a diameter in the millimetre range. These spots are no longer in a micrometre range; therefore, increasing the anodization time has no interest for this application.

It is noteworthy to mention that TiO_2 spots of micro and millimeter size with colors of brown and blue were obtained on a Ti plate by using the scanning droplet cell [8, 9]. This technique has been extensively used for generating oxide spots on different valve metals and for their characterization [37-39]. A discussion common to this technique and to the anodization tool presented in this work concerns the small droplet volume of electrolyte [34]. In the case of the scanning droplet cell, in an example concerning the oxidation of a Zirconium substrate, the capillary used for dispensing the electrolyte had a diameter of 150 µm, the droplet volume was about 0.2 nL and the oxide spots had a diameter of 150 µm and a thickness of about 15 nm. It has been suggested by the authors that the ratio of 1000 between the electrolyte volume and oxide volume is high enough in order to neglect possible changes of the electrolyte composition during the anodization. The anodization tool presented in this work has a diameter of 300 µm and the diameter of the central part of the obtained spots range from 450 µm to 750 µm with a thickness estimated from 30 to 100 nm. Following the same algorithm, a ratio varying from 10 to 100 between the electrolyte volume and the oxide volume is obtained in this work. This ratio would seem too low and possible considerable changes in the electrolyte composition could appear. These changes could be responsible of the morphology of the obtained TiO_2 layers that are nanoporous but are lacking of self-organized nanotubes as expected. Nevertheless it should be considered that the entire diameter of the spots was used for the calculation of this ratio, but, as described above, the center of spots seems more dense the that rest of the spot, and therefore the obtained ratio is probably underestimated. Changes in electrolyte composition were also discussed for anodization currents higher than $1A.cm^{-2}$ and an improvement of the scanning droplet cell that allows the electrolyte to flow was proposed [40]. In this work, the anodization currents (supplementary figure S5) are

considerably lower (in the order of 1 $\mu A.cm^{-2}$), therefore a flow of electrolyte seems not necessary. Nevertheless, an improvement of the anodization tool proposed here that would allow a flow of electrolyte could be achieved and a further study regarding the influence of this factor on the TiO_2 morphology is highly recommended.

A major difference between the example using scanning droplet cell for the anodization of Ti [8, 9] and the present work concerns the used electrolyte. While in the first case, an acetate buffer of pH 6 was used, an ethylene glycol based electrolyte was used in this work. The acetate buffer could compensate for a probable raise in pH due to the water reduction that appears at the gold counter electrode, whereas the ethylene glycol could not. This counter reaction could lead to changes in electrolyte viscosity and conductivity, parameters that could influence the morphology of TiO_2. Nevertheless, it is shown here that local anodization could be performed in organic electrolytes as well, even if the effect of the counter reaction is not well understood.

3.3. Oxygen detection during photocatalytic water oxidation at TiO_2 spots

The OF-UME allowed performing a second type of screening. In this second mode, the gold UME was used in combination with the local illumination by the optical fibre to detect directly the oxygen produced at the TiO_2 spots during the photocatalytic oxidation of water (Figure 2b) within the diffusion layer (~35 μm). Even if the UME was not exactly above the area under illumination, the UME is inside the O_2 diffusion layer generated above the substrate which makes this tool is perfectly suitable for a qualitative measurement that compare the O_2 generated on an array of spots.. Firstly, the OF-UME system was applied to record approach curves in substrate generator-tip collection mode (SG/TC). For this, a classical TiO_2 plate (obtained by anodization of a Ti plate at 50 V for 1 h) was used as the substrate for water photoelectrochemical oxidation (equation 4). The OF-UME was approached to this surface while the UME was used as an oxygen sensor (Figure 6). In the absence of the UV light, the TiO_2 substrate is not oxidizing water to O_2 thus the current recorded at the UME corresponds only to the reduction of oxygen dissolved in the solution (equation 5). In the presence of UV, the TiO_2 surface oxidises water to O_2. As the tip approaches to the substrate, it collects an increasing amount of oxygen produced by the substrate and the reduction current increases. The fitting of these curves with a theoretical model is not recommended as the measured response is not very sensitive to tip-substrate distance for the SG/TC mode [41]. Therefore, this experiment has only a qualitative value and was performed to confirm the effective operation of the newly designed OF-UME tool.

$$\text{At the } TiO_2 \text{ surface: } \quad 2H_2O + 4h^+ \rightarrow O_2 + 4H^+ \qquad (4)$$

At the OF-UME tip: $O_2 + 4H_2O + 4e^- \rightarrow 4HO^-$ (5)

The OF-UME tool was then used to measure the oxygen produced during the photoelectrochemical oxidation of water at one TiO_2 spot. As mentioned, the versatility of this dual tool allows the simultaneous imaging of the photocatalytic activity (Figure 7a) and of the produced oxygen (Figure 7b) at the very close proximity of the surface. Both mapping modes provide very good spatial resolutions with matching features, as it can be seen in Figure 7. Nevertheless, the time required for this imaging is rather long as the scan rate was 10 µm s^{-1}. Therefore, the OF-UME was further used as a local sensor in a static manner to detect the oxygen produced at all TiO_2 spots in a shorter time. For this, the tip was positioned on the centre of each spot, identified on the SECM image from Figure 3 and light-dark experiments were run as shown in Figure 8. It can be observed that the intensity of the current corresponding to oxygen reduction (Figure 8a) is proportional to the anodization potential. This is correlated also to the photocurrent obtained simultaneously on the TiO_2 spots (Figure 8b). Hence the amount of produced oxygen can be conveniently correlated with the photocatalytic properties of the TiO_2 spots. Useful information can be extracted from the transient light/dark experiments. For example, the tip-surface distance *d* can be extracted from these data. The time required for dioxygen to diffuse from the substrate to the tip is correlated to tip-substrate distance as follows: $d = \sqrt{Dt}$, where D is the diffusion coefficient of dioxygen in water (2.26 x 10^{-9} m^2 s^{-1}) [42]. This time could be measured from the moment when the light is turned on until the moment where the tip current decreases due to the oxygen reduction current (inset Figure 8a). The obtained value was around 0.5 s that corresponds to a tip-substrate distance of about 35 µm, which is a typical value for such an SECM experiment.

Combining the remarkable properties of an UME and an optical fibre in the same tool gives the possibility to illuminate the substrate on site right under the electrode. This is a better alternative to the use of an external UV source because the electrode could cast a shade on the substrate. For example, Zigah *et al.* showed how photoelectrogenerated hydroxyl radicals generated by a classical TiO_2 surface can be investigated using surface interrogation-SECM [24]. The authors have used a classic disk gold UME with an external UV source but the same study could be envisaged with the OF-UME described here. Kemp *et al*. used a silver disk UME and an external UV source to investigate the photomineralisation of 2,4-dichlorophenol at a classic TiO_2 surface [43]. In their work Sakai *et al*. used a carbon disk UME and an external

UV source to investigate chloride oxidation at a classic TiO_2 surface [44]. The same configuration was used by Simpson *et al*. to quantify the photogenerated adsorbed intermediates during the photo-assisted water oxidation reaction on lightly n-doped $SrTiO_3$ [17].

Other alternative tools that allow scanning of photoelectrochemical properties of libraries of semi-conductors have already been proposed. One example is the optical fibre surrounded by a ring electrode [30, 45, 46]. The construction of such tool requires sputtering of the gold electrode on the optical fibre and the electrical connection was achieved with anodic electrophoretic paint. Another very recent example is the photoelectrochemical scanning droplet cell microscopy (PE-SDCM) that is an upgrade to classical scanning droplet cell obtained by the integration of a light source for local illumination [47-49]. While these tools are well characterized, their construction requires either multiple laborious steps or 3D printing, the OF-UME tool described in this work is much easier to fabricate as it requires only the usual equipment and procedures used for a UME fabrication.

4. Conclusions

In conclusion, this work presents a tool, the CAP-UME that allows to locally anodize a Ti surface for the first time in an organic electrolyte at the micrometre range. This device, composed of a microcapillary and a gold microelectrode, is applied to the formation of arrays of TiO_2 spots with different physicochemical characteristics by tuning simple experimental parameters such as the potential and time of anodization. A second original tool, the OF-UME, based on a combination of an optical fibre with a gold UME was fabricated to probe these arrays. This device allows the simultaneous: *i*) photocurrent screening of the TiO_2 spots; *ii*) and sensing of the oxygen production using the gold UME. The tool benefits from the local illumination by the fibre that assures the on-site water oxidation and oxygen production. A direct correlation between the morphology of the TiO_2 spots, photocatalytic current and oxygen production was found. As a perspective, the gold electrode of the OF-UME tool could be used to control precisely the tool-substrate distance and thus the relation between distance and film morphology could be studied in-depth. This will probably lead to TiO_2 nanotubes micropattern that could present enhanced conversion energy in solar microcells.

Acknowledgements

The authors thank the PEPS NANO-GLOS and IDEX Bordeaux for the financial support.

References

[1] B. O'Regan, M. Grätzel, *Nature* **1991**, *353*, 737-740.
[2] K. Shankar, J. I. Basham, N. K. Allam, O. K. Varghese, G. K. Mor, X. Feng, M. Paulose, J. A. Seabold, K.-S. Choi, C. A. Grimes, *The Journal of Physical Chemistry C* **2009**, *113*, 6327-6359.
[3] M. R. Hoffmann, S. T. Martin, W. Choi, D. W. Bahnemann, *Chemical Reviews* **1995**, *95*, 69-96.
[4] A. L. Linsebigler, G. Lu, J. T. Yates, *Chemical Reviews* **1995**, *95*, 735-758.
[5] M. Valetaud, G. Loget, J. Roche, N. Hüsken, Z. Fattah, V. Badets, O. Fontaine, D. Zigah, *Journal of Chemical Education* **2015**, *92*, 1700-1704.
[6] R. J. M. Vullers, M. Ahlskog, C. Van Haesendonck, *Applied Surface Science* **1999**, *144–145*, 584-588.
[7] O. Ozcan, W. Hu, M. Sitti, J. Bain, D. S. Ricketts, *IET Micro Nano Letters* **2014**, *9*, 332-336.
[8] J. P. Kollender, A. I. Mardare, A. W. Hassel, *Electrochimica Acta* **2015**, *179*, 32-37.
[9] A. I. Mardare, A. D. Wieck, A. W. Hassel, *Electrochimica Acta* **2007**, *52*, 7865-7869.
[10] R. J. Collins, H. Shin, M. R. DeGuire, A. H. Heuer, C. N. Sukenik, *Applied Physics Letters* **1996**, *69*, 860-862.
[11] Y. Masuda, W. S. Seo, K. Koumoto, *Langmuir* **2001**, *17*, 4876-4880.
[12] M. Bartz, A. Terfort, W. Knoll, W. Tremel, *Chemistry-a European Journal* **2000**, *6*, 4149-4153.
[13] G. K. Mor, O. K. Varghese, M. Paulose, K. Shankar, C. A. Grimes, *Solar Energy Materials and Solar Cells* **2006**, *90*, 2011-2075.
[14] N. Casillas, P. James, W. H. Smyrl, *Journal of The Electrochemical Society* **1995**, *142*, L16-L18.
[15] W. Kylberg, A. J. Wain, F. A. Castro, *The Journal of Physical Chemistry C* **2012**, *116*, 17384-17392.
[16] H. S. Park, K. E. Kweon, H. Ye, E. Paek, G. S. Hwang, A. J. Bard, *The Journal of Physical Chemistry C* **2011**, *115*, 17870-17879.
[17] B. H. Simpson, J. Rodríguez-López, *Journal of the American Chemical Society* **2015**, *137*, 14865-14868.
[18] C. Amatore, C. Pebay, L. Thouin, A. Wang, J.-S. Warkocz, *Analytical Chemistry* **2010**, *82*, 6933-6939.
[19] S. So, K. Lee, P. Schmuki, *Journal of the American Chemical Society* **2012**, *134*, 11316-11318.
[20] A. J. Bard, F. R. F. Fan, J. Kwak, O. Lev, *Analytical Chemistry* **1989**, *61*, 132-138.
[21] X. Chen, S. S. Mao, *Chemical Reviews* **2007**, *107*, 2891-2959.
[22] D. Gong, C. A. Grimes, O. K. Varghese, W. Hu, R. S. Singh, Z. Chen, E. C. Dickey, *Journal of Materials Research* **2001**, *16*, 3331–3334.
[23] P. Roy, S. Berger, P. Schmuki, *Angewandte Chemie-International Edition* **2011**, *50*, 2904-2939.
[24] D. Zigah, J. Rodríguez-López, A. J. Bard, *Physical Chemistry Chemical Physics* **2012**, *14*, 12764-12772.
[25] C. Kranz, *Analyst* **2013**, *139*, 336-352.
[26] C. Laslau, D. E. Williams, J. Travas-Sejdic, *Progress in Polymer Science* **2012**, *37*, 1177-1191.
[27] Y. Takahashi, A. I. Shevchuk, P. Novak, Y. Murakami, H. Shiku, Y. E. Korchev, T. Matsue, *Journal of the American Chemical Society* **2010**, *132*, 10118-10126.
[28] Y. Takahashi, A. I. Shevchuk, P. Novak, Y. Zhang, N. Ebejer, J. V. Macpherson, P. R. Unwin, A. J. Pollard, D. Roy, C. A. Clifford, H. Shiku, T. Matsue, D. Klenerman, Y. E. Korchev, *Angewandte Chemie-International Edition* **2011**, *50*, 9638-9642.
[29] K. Lee, A. Mazare, P. Schmuki, *Chemical Reviews* **2014**, *114*, 9385-9454.
[30] Y. Lee, A. J. Bard, *Analytical Chemistry* **2002**, *74*, 3626-3633.
[31] P. James, *Journal of The Electrochemical Society* **1996**, *143*, 3853.
[32] M. V. Diamanti, B. Del Curto, M. Pedeferri, *Color Research & Application* **2008**, *33*, 221-228.
[33] E. Gaul, *Journal of Chemical Education* **1993**, *70*, 176.
[34] A. Moehring, M. M. Lohrengel, *Electrochemical Society Proceedings* **1999**, *42*, 114-121.
[35] R. A. Said, *Journal of The Electrochemical Society* **2003**, *150*, C549-C557.
[36] J. M. Macak, K. Sirotna, P. Schmuki, *Electrochimica Acta* **2005**, *50*, 3679-3684.

[37] A. W. Hassel, M. M. Lohrengel, *Electrochimica Acta* **1997**, *42*, 3327-3333.
[38] M. M. Lohrengel, A. Moehring, M. Pilaski, *Electrochimica Acta* **2001**, *47*, 137-141.
[39] M. Pilaski, M. M. Lohrengel, *Electrochimica Acta* **2003**, *48*, 1309-1313.
[40] M. M. Lohrengel, C. Rosenkranz, I. Klüppel, A. Moehring, H. Bettermann, B. V. d. Bossche, J. Deconinck, *Electrochimica Acta* **2004**, *49*, 2863-2870.
[41] F.-R. F. Fan, B. Liu, J. Mauzeroll, in *Handbook of Electrochemistry* (Ed.: C. G. Zoski), Elsevier, Amsterdam, **2007**, pp. 471-XIII.
[42] G. A. Snook, N. W. Duffy, A. G. Pandolfo, *Journal of the Electrochemical Society* **2008**, *155*, A262-A267.
[43] T. J. Kemp, P. R. Unwin, L. Vincze, *Journal of the Chemical Society, Faraday Transactions* **1995**, *91*, 3893-3896.
[44] H. Sakai, R. Baba, K. Hashimoto, A. Fujishima, *Journal of Electroanalytical Chemistry* **1994**, *379*, 199-205.
[45] K. Maruyama, H. Ohkawa, S. Ogawa, A. Ueda, O. Niwa, K. Suzuki, *Analytical Chemistry* **2006**, *78*, 1904-1912.
[46] H. Ye, J. Lee, J. S. Jang, A. J. Bard, *The Journal of Physical Chemistry C* **2010**, *114*, 13322-13328.
[47] J. P. Kollender, B. Gallistl, A. I. Mardare, A. W. Hassel, *Electrochimica Acta* **2014**, *140*, 275-281.
[48] J. Gasiorowski, J. P. Kollender, K. Hingerl, N. S. Sariciftci, A. I. Mardare, A. W. Hassel, *Physical Chemistry Chemical Physics* **2014**, *16*, 3739.
[49] J. P. Kollender, A. I. Mardare, A. W. Hassel, *ChemPhysChem* **2013**, *14*, 560-567.

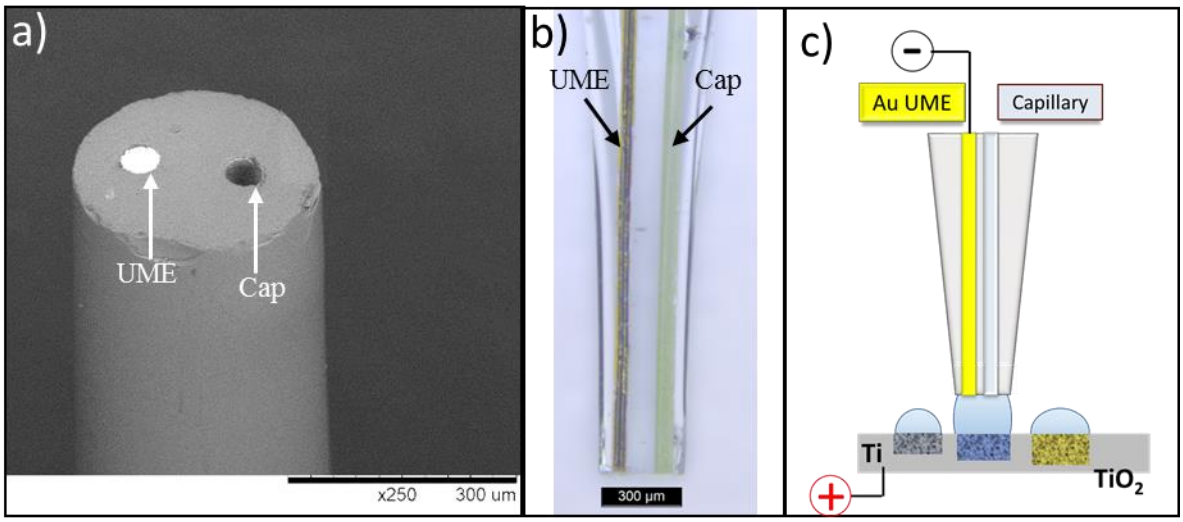

Figure 1. a) Scanning electron microscopy (SEM) image of the microcapillary-ultramicroelectrode (Cap-UME) tool used for the local anodization of Ti; b) Optical image of the side view of the Cap-UME tool; c) Scheme of the local anodization of Ti plate for the generation of multiple TiO_2 spots.

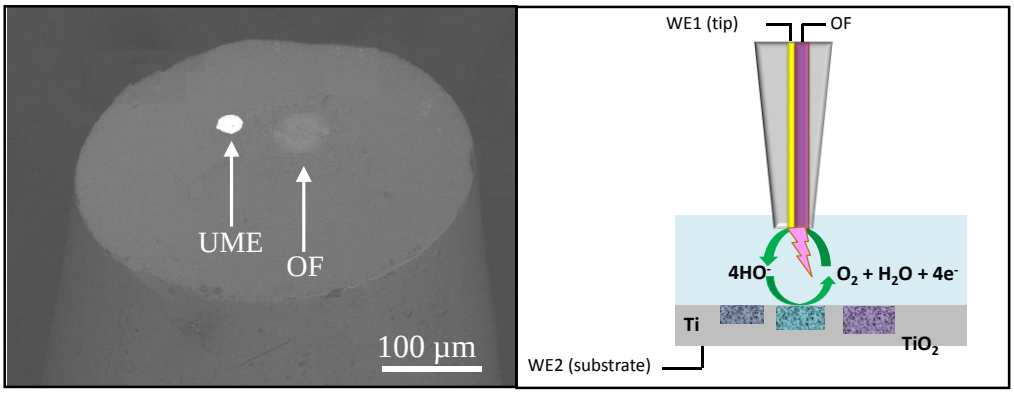

Figure 2. a) SEM image of the dual OF-UME probe; b) Scheme of the simultaneous screening of TiO_2 spots for photoelectrochemical water oxidation and for oxygen reduction using the OF-UME tool.

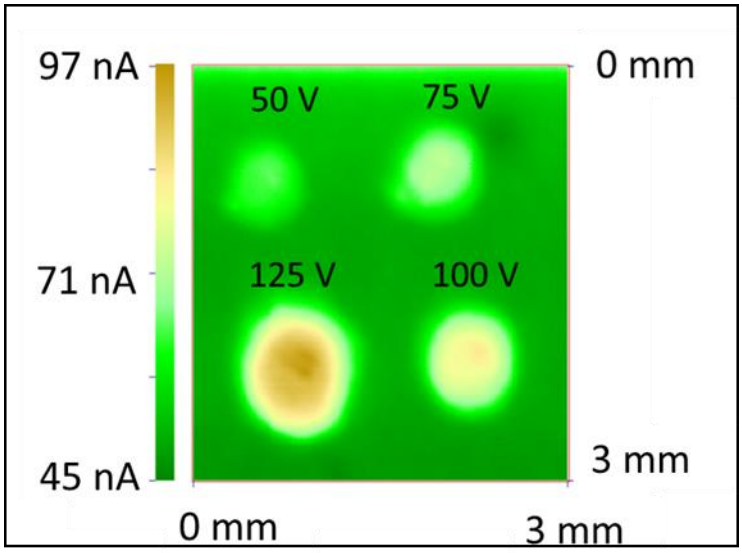

Figure 3. SECM image of the TiO_2 spots. Experimental conditions: air equilibrated NaOH 1 M, E_{sub} = 0.5 V *vs* Ag/AgCl, under UV illumination, 100 mW cm^{-2}; scan rate of the optical fiber 400 µm s^{-1}.

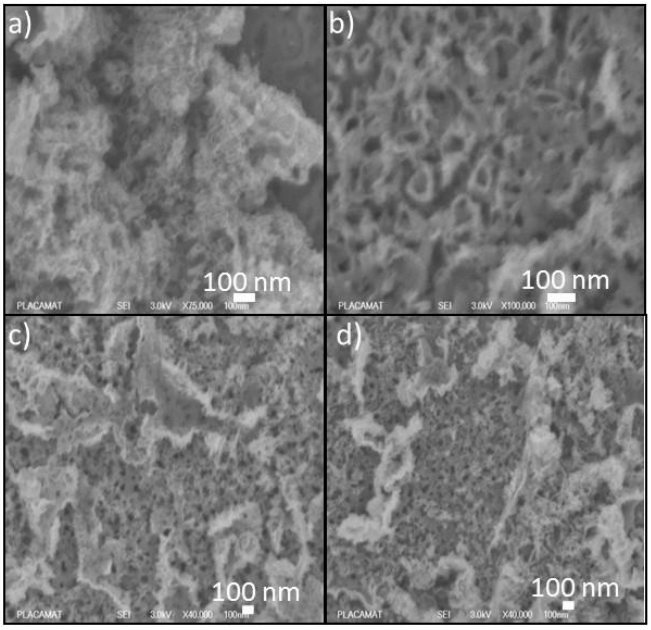

Figure 4. SEM images of TiO_2 spots produced with different anodization potentials: a) 50 V, b) 75 V, c) 100 V, d) 125 V. Anodization time: 1 hour.

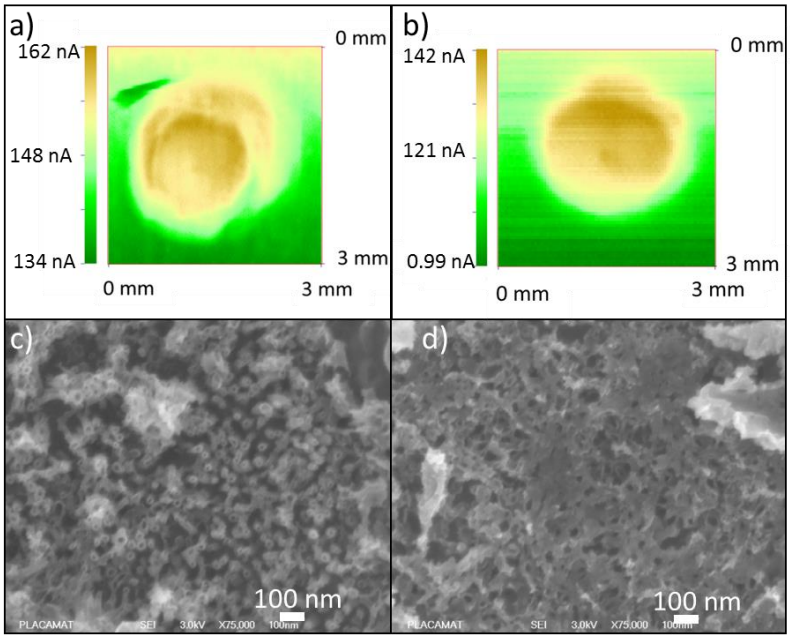

Figure 5. SECM and SEM images of TiO_2 spots produced at longer anodization times: 4 h at a) 50 V, b) 75 V. Experimental conditions: air equilibrated NaOH 1 M, E_{sub} = 0.5 V *vs* Ag/AgCl, under UV illumination, 100 mW cm^{-2}; scan rate of the optical fiber 400 µm s^{-1}.

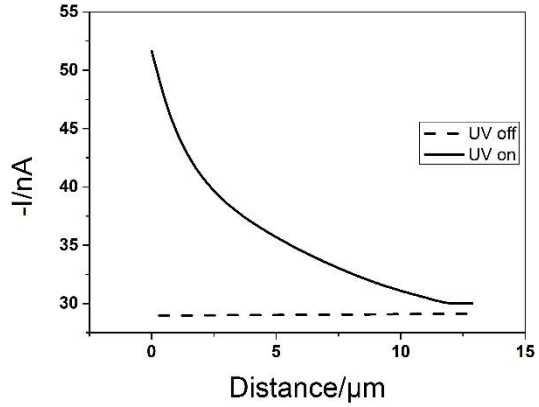

Figure 6. Approach curves in the SG-TC mode using the OF-UME tool. Experimental conditions: Ti plate anodized at 50 V for 1 h; illumination, 100 mW cm^{-2}, air equilibrated 1 M NaOH, E_{UME} = -0.4 V *vs* Ag/AgCl, E_{sub} = 0.5 V *vs* Ag/AgCl.

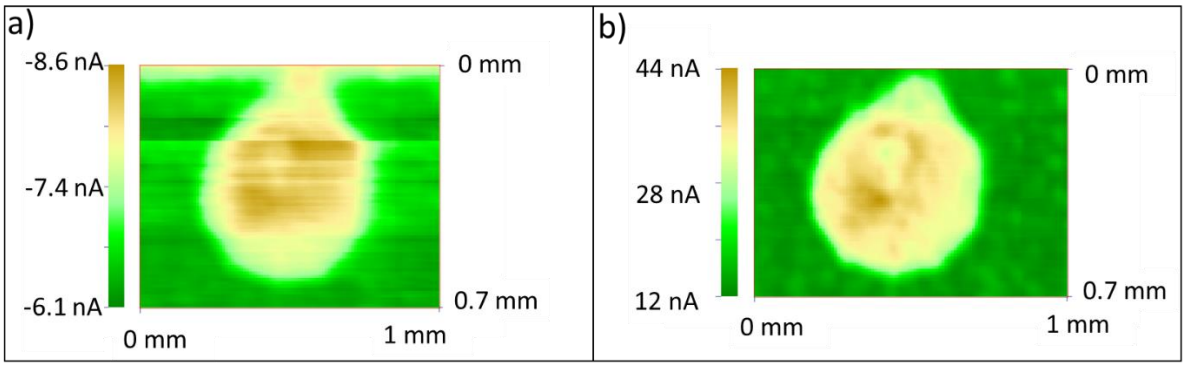

Figure 7. SECM images of a) the photocurrent on TiO_2 spot and b) of oxygen reduction on the gold UME of the dual tool. Experimental conditions: TiO_2 spot obtained with the Cap-UME tool; anodization potential, 50 V; anodization time 1 h. SECM experimental conditions: illumination, 100 mW cm^{-2} with the fibre part of the OF-UME tool; electrolyte, air equilibrated 1 M NaOH; E_{UME} = -0.4 V *vs* Ag/AgCl; E_{sub} = 0.5 V *vs* Ag/AgCl; scan rate of the optical fiber, 10 μm s^{-1}.

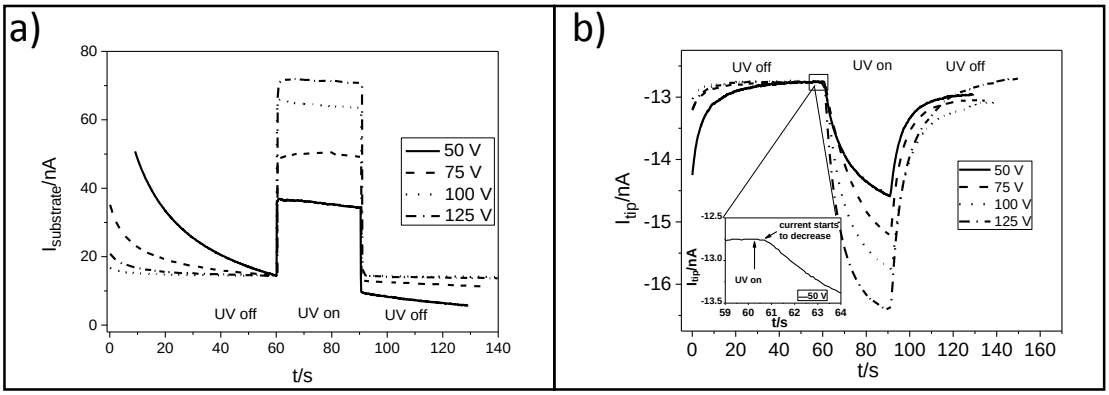

Figure 8. Light-dark experiments on several TiO_2 spots produced with different anodization potentials**:** a) photocatalytic water oxidation current recorded on the TiO_2 spots; b) O_2 reduction current recorded with the OF-UME. Experimental conditions: illumination, 100 mW cm^{-2}, air equilibrated 1 M NaOH, E_{UME} = -0.4 V *vs* Ag/AgCl, E_{sub} = 0.5 V *vs* Ag/AgCl.